JMEPEG (2007) 16:113–118
DOI: 10.1007/s11665-006-9018-7

1059-9495/$19.00

Reticulated Porous Multiphase Ceramics with Improved Compressive Strength and Fracture Toughness

Shou-ren Wang, Hao-ran Geng, Lin-hai Hui, and Ying-zi Wang

(Submitted September 24, 2005; in revised form April 03, 2006)

A multiphase reticulated porous ceramic (RPC) as Si_3N_4–Al_2O_3–SiO_2 was fabricated by replication techniques. Proper volumes of additives and twice sinter- twice immerse process endow the RPC an excellent crack healing and submerging property. The compressive strength and fracture toughness improved owing to the crack bridging behavior. The existence of pores in struts in RPC blunt the crack tip and increased the external force needed to propagate the crack. The mechanisms play a beneficial role in enhancing the compressive strength and fracture strength. Si_3N_4 RPC with additives of 5%Al and 5% Al_2O_3 yielded the compressive strength of 9.8 MPa and fracture toughness of 0.3 MPa $m^{1/2}$.

Keywords compressive strength, crack bridging, crack healing, crack tip blunting, fracture toughness, reticulated porous ceramic

1. Introduction

Due to their unique properties such as low density, high thermal shock resistance, low thermal and electrical conductivity, high permeability, high temperature stability and high resistance to chemical attack (Ref 1-4), reticulated porous ceramics (RPC) have found increasing applications in the fields of molten metal processing, diesel engine exhaust filters, catalyst supports and reinforcement of metal matrix composites as well as lightweight structural components.

RPC can be fabricated by a variety of methods, the most common of which is the replication technique (Ref 5) and is also called the "polymeric sponge" process (Ref 6). However, some drawbacks of RPC made by this method were low compressive strength, low inter density of the cells, hollow struts, and residual cracking in struts of foam after burnout of the polymer substrate, which has not been wholly overcome. Particularly, the cracks in the struts are lethal to the mechanical properties of RPC. Therefore, investigation of crack mechanisms such as crack resistance, crack bridging, and crack arrest as well intrinsic crack growth and closure behavior is very important for the development and application of RPC.

In this article, a reticulated porous multiphase ceramic (Si_3N_4–Al_2O_3–SiO_2) was fabricated through a double sintering and immersion process. The process, different from the once sintering and immersion process, was found to be the most effective method to improve the mechanical properties. Silicon nitride was used as a candidate material to make RPC with high strength, excellent oxidation resistance, low thermal expansion coefficient, and high fracture toughness. (Ref 7-10) As a low temperature-sintering additive, Al would melt and be oxidize into Al_2O_3 in the course of sintering. The oxide decreases the driving force of crack extension. As high temperature sintering additives, Al_2O_3 would improve the density of struts and increase the crack closure stresses. In-situ SiO_2 phase would form at high temperature and in an oxidizing atmosphere, so Al_2O_3 (oxidation + addition) and SiO_2 (oxidation + in-situ) will emerge as second and third ceramic phases in RPC. The above fabrication technique not only improved the compressive strength and fracture toughness, and increased the density of struts and removed the crack in struts, but also arrested and bridged cracks and blunted the crack-tip in struts of RPC.

S. Wang, School of Mechanical Engineering, Ji'nan University, Jinan 250022, P.R. China; **S. Wang,** The Key Laboratory of Liquid Structure and Heredity of Materials of Shandong University, 250014 Ji'nan, P.R. China; and **H. Geng, L. Hui** and **Y. Wang,** School of Material Science, Ji'nan University, 250022 Ji'nan, P.R. China; Contact e-mail: strong_422@163.com.

2. Experimental Procedure

2.1 Materials

A commercial β-Si_3N_4 powder ($Si_3N_4 \geq 97\%$, diameter $\leq$ 100 μm, Shanghai Silicon Materials Plant, China) was used as starting material. Aluminum fine powder ($Al \geq 99.26\%$, $D_{50} = 4 \pm 1.5$ μm, Shandong Aluminum Industry Company, China) as sintering additive was mixed with the starting material and ball-milled for 4 h using Al_2O_3 balls. Silica sol as a cohesive agent was added in the powder mixture. The mixed slurry was stirred for 2 h. A commercial silica sol (SiO_2, 30.0–31.0%; pH, 8.5–10.0, Shanghai Kenning Silica Sol Company, China) was used as a binder and a surfactant carboxymethyl cellulose was added to serve as a wetting agent. Kaolin (Sino Surplus International Limited, Beijing, China) and bentonite (Nanhua Hongshan Bentonite Company, Liaoning, China) were added to improve the rheology of the slurry (contents shown in Table 1).

Commercial polyurethane sponges (PUS, Shanghai Nanjia Sponges Production Company, China) with reticulated structure, interconnected struts and open porosity of approximately 10 pores per inch were chosen in this study. The PUS was

Table 1 The contents of sintering additives

Sample	Aluminium, wt.%	Alumina, wt.%	Silica sol, wt.%	Kaolin, wt.%	Bentonite, wt.%	Carboxymethyl cellulose, wt.%	Silicon nitride, wt.%	Sintering process
A1	–	–	14.5	3.5	1	1	80	OSOI[a]
A2	5	5	14.5	3.5	1	1	70	OSOI
B1	5	5	14.5	3.5	1	1	70	TSTI[b]
B2	10	10	14.5	3.5	1	1	60	TSTI

[a]once sinter - once immerse process [b]twice sinter - twice immerse process

Table 2 The contents of suspending liquid

Sodium oxide, wt.%	Sodium Metasilicate, wt.%	Silica sol, wt.%	Silicon oxide, wt.%, D_{50} = 10 μm
2	2	26	70

cleaned with de-ionized water before impregnation and cut into approximately 100×30×30 mm samples. The PUS was then immersed into the homogeneous ceramic slurry for about 10 min and compressed continually. The impregnated sponges passed through a preset roller to remove excess slurry. The optimum roller separation corresponds to about 20% of the thickness of the sponges and two passages are specially determined to remove the excess slurry (Ref 11). Subsequently, the samples were put into a rotating cylinder to obtain uniformity of struts attached by the slurry and avoid jamming the mesh of reticulated PUS by the action of centrifugal force. The rotation process is an important procedure to obtain high-open porous ceramic reinforcement. The samples were then placed in a drying oven at 160 °C for at least 20 h.

Firing of the specimen was conducted in a programmable box furnace. First, the samples were heated to 660 °C at a rate of 50 °C/h to burn away the PUS framework; second, the samples were heated to 1000 °C at 200 °C/h and maintained at the temperature for 60 min. Third, the samples were immersed into a suspending liquid (contents of which are shown in Table 2) for 2 h and put into the rotating cylinder and then dried for 20 h at 160 °C. To prevent the samples' mesh of ceramic foam from being jammed, the suspending liquid used in the second immersion should have lower concentration than that of the slurry used in the first immersion. Subsequently, the samples were heated to 1400 °C at 200 °C/h and held for 60 min at 1400 °C for sintering of the ceramic powder.

2.2 Characterization

The morphologies and fracture surface characteristics of RPC were characterized by a scanning electron microscope (SEM, Hitachi, No.S-2500). The density and porosity were measured using Archimedes measurements (ASTM C373). The phase composition of RPC was observed by standard powder X-ray diffraction (XRD, Bruker D8, Germany). The chemical compositions were determined by the energy spectrum analyses (ESA, OXFOED INCA). The compressive strength and fracture toughness were measured using an Instron 1195 universal testing machine with a cross-head speed of 0.5 mm min^{-1}. Fracture toughness was measured by a single-notched-beam technique. The pore size and effective grain width at the crack tip were measured by a line intercept method (Ref 12).

3. Results

During the entire sintering process, some cavities, which were earlier occupied by PUS occurred in the center of the struts. Lower heating rate should be adopted to avoid cracking of the struts during the volatilization of PUS framework. The strength of RPC is affected more by the presence of cracks in the struts than by the presence of a central void. The samples sintered by twice sinter- twice immerse process have better microstructure than that sintered by the once sinter- once immerse process. Figure 1 shows the cross-section micrographs of samples A1, A2 and B1 (SEM).

In the first stage of the adopted twice sinter-twice immerse process, Al powder would be oxidized with increasing of sintering temperature. The liquid Al will diffuse in the solid phases and heal the initial cracks. With the increases of Al content, the crack arrest ability increased gradually. During the second sintering stage, the additives of Al_2O_3 and SiO_2 (some from silica sol and some from in-situ oxidation of Si_3N_4) produce a glass phase at temperatures above 1200 °C (Ref 13). The glass phase has a good effect on the densification of RPC (Ref 14). Figure 1(a) shows the surface micrograph of RPC with no additives and no twice sinter-twice immerse process. From Fig. 1, the surface of strut was rough and has no shine. Large cracks (arrowed) on the strut surface were observed. Moreover, a larger amount of micro-cracks were also observed at higher magnification (Fig. 1a). With more sintering additives, the cracks in the struts decrease in number owing to the driving power from liquid glass phase at high sintering temperatures(Fig. 1b), but still there are some large cracks in the struts(arrowed). With the twice sinter-twice immerse process and with Al 5 % , Al_2O_3 5% sintering additives added, as shown in Fig. 1(c), more glass phases formed and covered the Si_3N_4 grains, so the surface of struts was bright and slick. Figure 2 shows the cross-section micrograph of strut of sample A2. The surface of the strut was covered by an Al_2O_3 + SiO_2 boundary layer that was examined by the energy spectrum analyses (ESA, OXFOED INCA) (Point-3). While in the interior of the struts, there are mainly Si_3N_4 grains (Point-1), with the increase of distance from center to the surface of the strut, there is more Al than less Si (Point-2).

The compressive strength of sample A_1, A_2, B_1 and B_2 are 4 MPa, 6.2 MPa, 9.8 MPa and 6.1 MPa, respectively (Fig. 3). The fracture toughness of sample A_1, A_2, B_1 and B_2 are 0.1 MPa $m^{1/2}$, 0.15 MPa $m^{1/2}$, 0.3 MPa $m^{1/2}$ and 0.18 MPa $m^{1/2}$, respectively (Fig. 4). From Figs. 3 and 4, it is seen that whereas appropriate additives increase the fracture toughness and ensure enough the compressive strength of RPC, excessive amounts of additives have adverse influence on the properties.

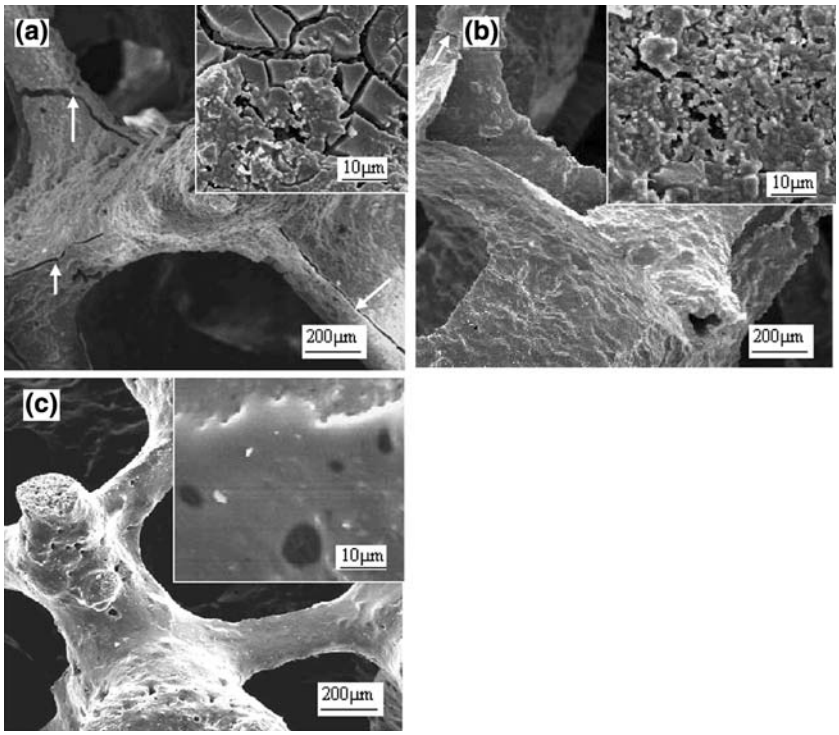

Fig. 1 SEM views of surface of samples (a, sample A1; b, sample A2; c, sample B1)

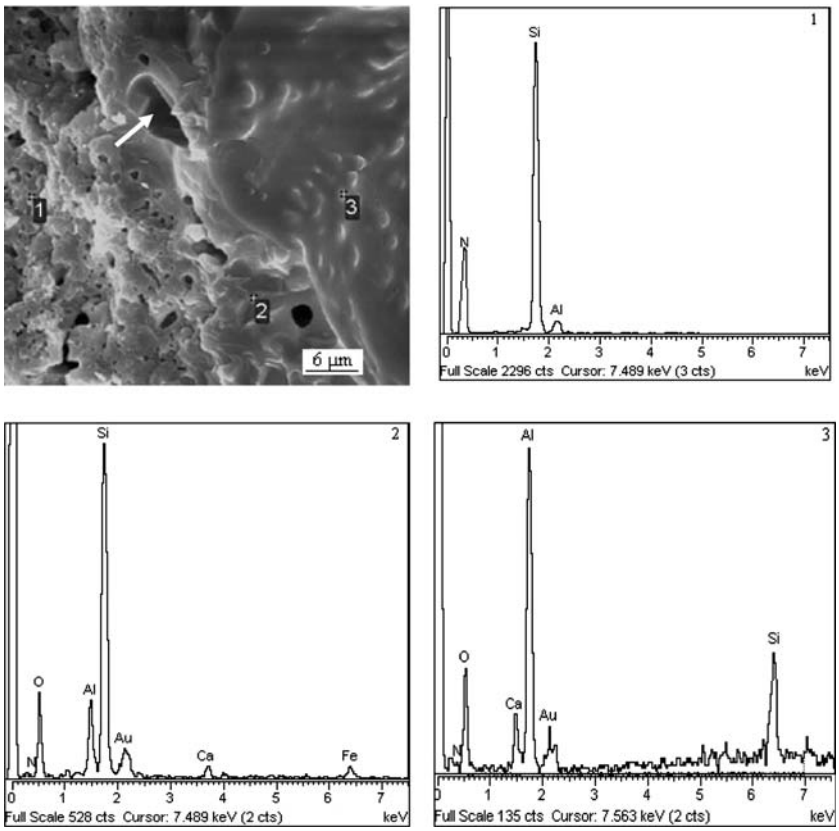

Fig. 2 The cross-section micrographs of struts of RPCs (A2) and its chemical composition

4. Discussion

4.1 Crack Bridging and Closure Mechanism

Many factors such as porosity, sintering temperature, topology and geometry of structure of porous ceramic framework, cracks in the struts, uniformity of cell window, and particle sizes are decisive for the compressive strength and fracture strength of RPC. Higher compressive strength and fracture toughness can be achieved by removing the cracks in struts, decreasing the porosity, raising the sintering temperature properly, fabricating mean ceramic framework, and choosing pure precursor powders with fine particle sizes.

During the sintering process, PUS is burnt away and there occur some cavities in the struts of RPC. Some cavities were jammed by glassy phase that formed by delivering sintering, but still there were some cavities remaining in the struts (Fig. 2). These cavities have both positive and negative influences. The positive influence is that cavities become the tension releaser due to the stress dispersion and transfer. (crack-tip blunt mechanism). The negative influence is that the relative density of the strut would decrease owing to the existence of the cavities. The relative density parameter is one of the predominant factors for the improvement of the compressive strength and fracture toughness as shown by the following equations (Ref 15).

$$\sigma_{cs} = C_1 \sigma_{fs} \left(\frac{\rho^*}{\rho_s}\right)^{3/2} \quad \text{(Eq 1)}$$

$$K_{IC} = C_2 \sigma_{fs} \sqrt{\pi l} \left(\frac{\rho^*}{\rho_s}\right)^{3/2} \quad \text{(Eq 2)}$$

where σ_{cs} is the compressive strength, K_{IC} is the fracture toughness, σ_{fs} is the fracture module of solid material, $\frac{\rho^*}{\rho_s}$ is the relative density, l is the length of strut, C_1 and C_2 are constants. Green (Ref 16, 17) had measured the fracture toughness of brittle polymer foam, indicating that fracture toughness of reticulated porous materials follow Weibull distribution. Maiti and Ashby (Ref 18) used a polyhedral cell model to develop an analytical expression for the fracture toughness of RPC. The line shown in Fig. 5 is based on Maiti-Ashby model with $\sigma_{fs} = 591$ Mpa. The experimental data of the present work shown in Fig. 5 describe the variation of $K_{IC}/\sigma_{fs}\sqrt{\pi l}$ with increasing ρ^*/ρ_s and different volume additions of Al aznd alumina. With an increase of relative density, the fracture toughness was improved, and the numerical values of $K_{IC}/\sigma_{fs}\sqrt{\pi l}$ of sample B_1 were closest to the Maiti-Ashby model. The additives and twice sinter-twice immerse process endow the RPC an excellent crack healing and submerging property. The crack submerging mechanism including crack bridging and crack trapping help in removing the cracks which is Schematically shown in Fig. 6. With the increase of test temperature, the additive Al diffused inside the struts and on the strut surface melted were and oxidized. At the same time, Si_3N_4 powders were oxidized to SiO_2. Oxide nucleation occurred continually and so did grain growth (Fig. 6a). A SEM view of oxide growth in the crack is shown in Fig. 7. Especially the oxide grains distributed in crack tip reduce the critical crack opening displacement and prevent cracks from expanding (crack trapping). Crack trapping in crack fronts could improve the resistance to crack extending. Simultaneously, oxides begin to enter the channels of cracks, nails up and down connect each other eventually, forming a bridge (Fig. 6b). With more

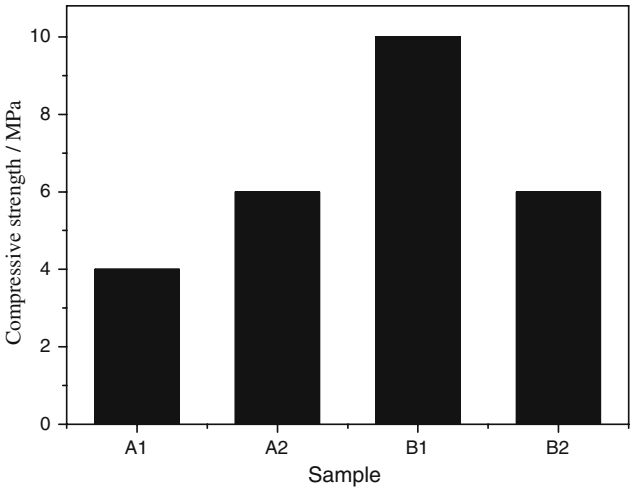

Fig. 3 Compressive strength of samples A1, A2, B1 and B2

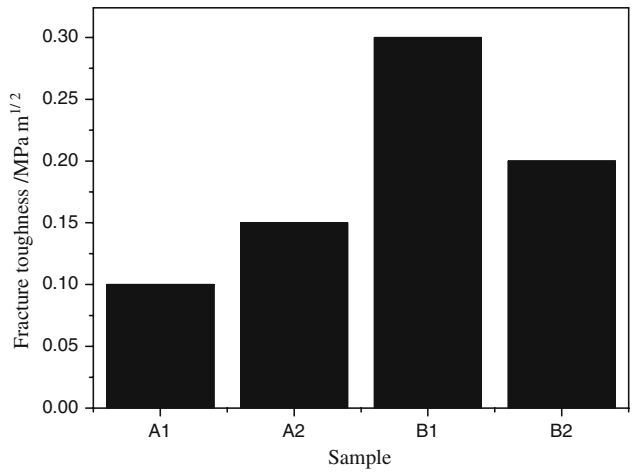

Fig. 4 Fracture toughness of samples A1, A2, B1 and B2

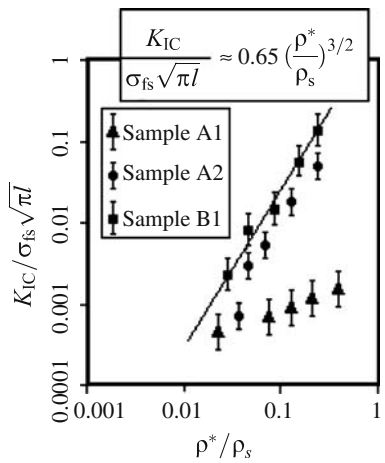

Fig. 5 The relation of $K^*_{IC}/\sigma_{fs}\sqrt{\pi l}$ and ρ^*/ρ_s

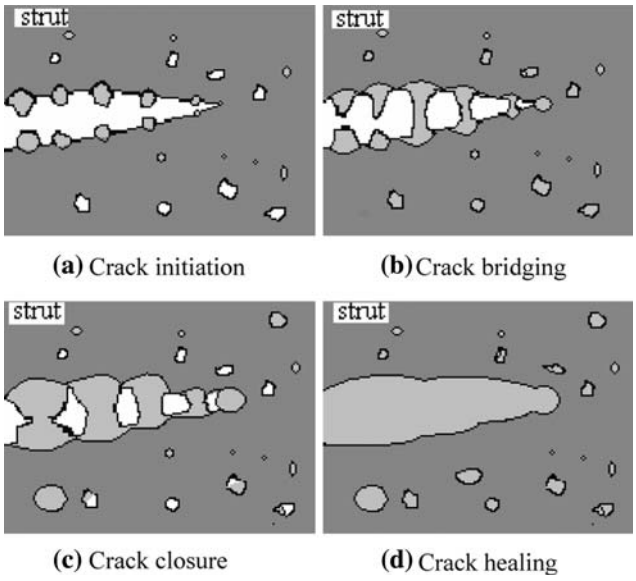

Fig. 6 Schematic representation of a bridged crack in struts of RPCs

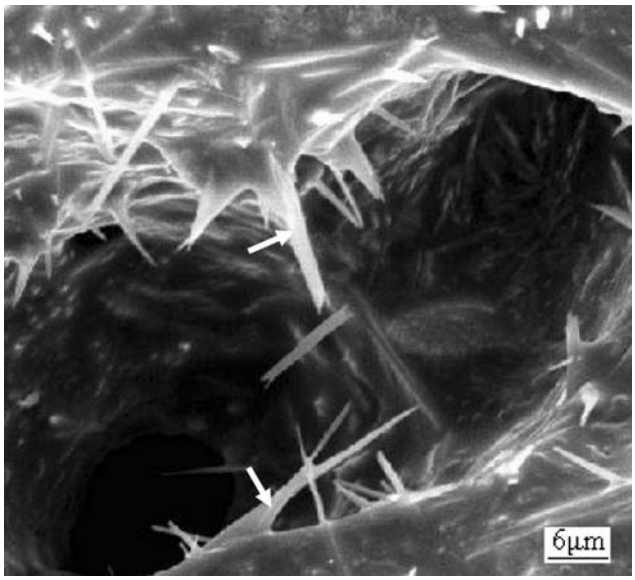

Fig. 7 SEM view showing oxide growth in cracks

oxidation taking place, the bridges turn wider so that the channels of cracks become narrower (Fig. 6c). This is the crack bridging mechanism for large cracks. The bridging unit improved lateral constraints on two sides of cracks. Finally, the channels of cracks and hollow struts were jammed completely (Fig. 6d). Especially, large amounts of micro-cracks were healed by this mechanism during high temperature process in fabricating RPC.

4.2 Crack-Tip Blunting Behavior

The above crack healing process usually occurs in the fabrication stage. Once cracks appear under external stresses, it is of importance to increase the crack growth resistance. Equations (1) and (2) did not deal with the

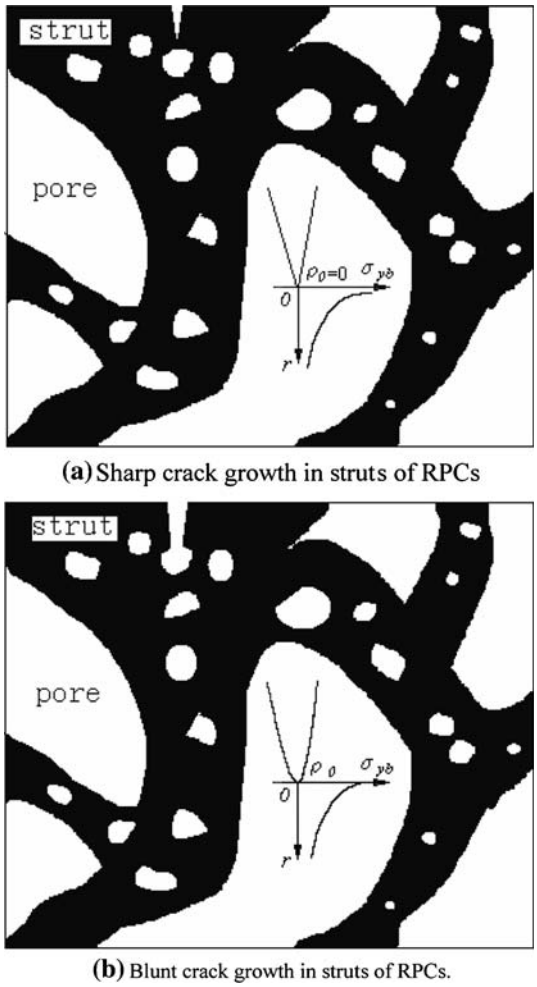

Fig. 8 Schematic representation of a crack propagated and a blunt crack-tip in RPCs

positive influence of cavities in struts of RPC. Theses cavities, to an extent, can make the crack blunt and increase the compressive strength and fracture toughness of RPC. The larger the pore size at the crack front, the higher the fracture toughness of RPC relative to their fracture strength (Ref 19). A crack-tip blunting model of RPC is proposed as follows (Ref 20, 21)

$$\sigma_{yb} = \frac{K_{Ib}}{\sqrt{2}} \frac{1 + \frac{\rho_0}{r}}{(1 + \frac{\rho_0}{2r})^{\frac{3}{2}}} \quad \text{(Eq 3)}$$

where ρ_0 is the root radius of the blunt crack, which is half of the pore width at the crack tip, r is the distance away from the crack tip, σ_{yb} is the solution of the stress on the r-axis (shown in Fig. 8) around a crack tip under a uniform tensile stress and K_{Ib} is the stress intensity factor at the blunt crack tip. It is expressed in Fig. 8, which is a schematic representation of a crack propagated and a blunt crack-tip in RPC. When a crack meets a cavity, the root radius value (ρ_0) increases, the tensile stress in the crack tip decreases, therefore, the crack tip becomes blunt and the stress-concentration is decreased at the crack tip. The external load to propagate the crack increases, therefore, the fracture toughness of RPC was enhanced. Deng (Ref 19) has also

investigated the crack-tip blunting mechanism of RPC and revised the above crack blunting model as

$$\frac{K_{Ib}}{K_{IC}} = (1 + \frac{\rho_0}{2r_0})^{1/2} \quad \text{(Eq 4)}$$

where r_0 is the characteristic zone corresponds to a maximum deviated grain arrangement at the crack front. This model indicated that the crack-tip blunting obviously increases the fracture toughness of porous ceramics and that the larger the pore size at the crack front, the higher the fracture toughness of the porous ceramics. The experimental data of present work prove the validity of this theoretical prediction.

5. Conclusions

1. As a low temperature sintering additive, Al melted and oxidized into Al_2O_3 in the course of sintering and jammed the hollow struts. Al_2O_3 as a high temperature sintering additive improved the density of struts. In-situ SiO_2 phase was formed at high temperature and in an oxidizing atmosphere. Multiphase RPC as Si_3N_4–Al_2O_3–SiO_2 were fabricated.
2. Appropriate volumes of Al and Al_2O_3 additives in Si_3N_4 RPC increase the density of struts and arrest the initiation of cracks. The twice sinter-twice immerse process was carried out in order to ensure the improvement of the compressive strength and fracture toughness. Si_3N_4 RPC with additives of 5%Al and 5%Al_2O_3 respectively yielded the compressive strength of 9.8 MPa and a fracture toughness of 0.3 MPa $m^{1/2}$.
3. The additives and the TWICE SINTER-TWICE IMMERSE process endow the RPC excellent crack healing and submerging properties including crack bridging and crack trapping. The existence of some pores in struts of RPC blunted the crack tip. These mechanisms play a beneficial role in enhancing the compressive strength and fracture strength.

Acknowledgments

This work was supported by the Natural Science Foundation of Shandong province (**Y2006F03**). Part of this research was done at the Institute of Materials Science and Technology of Jinan University. The authors are owing a debt of gratitude to the technical staff of these two institutions for their help.

References

1. R.W. Rice, Summary of porosity and micro-cracking applications, special fabrication, and engineering. *Porosity of Ceramics*, Chapter 10, Ed., Marcel Dekker, New York, 1998
2. E.J.A.E. Williams and J.R.G. Evans, Expanded Ceramic Foam, *J. Mater. Sci.*, 1996, **31**, p 559–563
3. S.B. Bhaduri, Science and Technology of Ceramic Foams, *Adv. Performance Mater.*, 1994, **1**, p 205–220
4. L.M. Sheppard, Porous Ceramics: Processing and Application, *Ceram. Trans.*, 1993, **31**, p 2–3
5. K. Schwartzwalder and A.V. Somers, Method of Making Porous Ceramic Articles, U.S. Patent 3090094, 1963
6. J. Saggio-Woyaansky and C.E. Scottetal, Processing of Porous Ceramics, *Am. Ceram. Soc. Bull.*, 1992, **71**(11), p 1674–1682
7. S.P. Taguchi and S. Ribeiro, Silicon Nitride Oxidation Behaviour at 1000 and 1200 ºC, *J. Mater. Process. Technol.*, 2004, **147**, p 336–342
8. A. Rosenflanz, Silicon Nitride and Sialon Ceramics, *Curr. Opin. Solid State Mater. Sci.*, 1999, **4**, p 453–459
9. J.P. Sancho, J.A. Pero-Sanz, and L.F. Verdeja, Toughness of Si[3]N[4] Ceramics Obtained by Precipitating Sintering Aids as Hydroxides, *Mater. Character.*, 2003, **50**, p 11–22
10. D.Y. Chen, B.L. Zhang, and H.R. Zhang, Combustion Synthesis of Network Silicon Nitride Porous Ceramics, *Ceram. Int.*, 2003, **29**, p 363–364
11. X. Zhu, D. Jiang, and S. Tan, The Control Of the Slurry Rheology in the Processing of Reticulated Ceramics, *Mater. Res. Bull.*, 2002, **37**, p 541–553
12. Z.Y. Deng, J.L. Shi, Y.F. Zhang, T.R. Lai, and J.K. Guo, Creep and Creep Recovery Behavior on Silicon-Carbide-Particle-Reinforced Alumina, *J. Am. Ceram. Soc.*, 1999, **82**, p 944–952
13. G.W. Han, D. Feng, and M. Yin, Ceramic/Aluminum Co-Continuous Composite Synthesized by Reaction Accelerated Melt Infiltration, *Mater. Sci. Eng. A*, 1997, **225**(1–2), p 204–207
14. S. Natansohn, A.E. Pasto, and W.J. Rourke, Effect of Powder Surface. Modifications on the Properties of Silicon Nitride Ceramics, *J. Am. Ceram. Soc.*, 1993, **76**(9), p 2273–2284
15. L.J. Gibson and M.F. Ashby, *Cellular Solids, Structure and Properties*. University Press, Cambridge, 1999
16. D.J. Green, Fabrication and Mechanical Properties of Lightweight Ceramics Produced by Sintering of Hollow Spheres, Final Report on AFOSR contract No.F49620-83-C0078, 1984
17. D.J. Green, *J. Am. Ceram. Soc.*, 1983, **66**, p 288–292
18. K. Maiti, M.F. Ashby, and L.J. Gibson, Fracture Toughness of Brittle Cellular Solids, *Scripta Metallurgica.*, 1984, **18**, p 213–217
19. Z.Y. Deng, J. She, Y. Inagaki, F.J. Yang, T. Ohji, and Y. Tanaka, Re-inforcement by Crack-Tip Blunting in Porous Ceramics, *J. Eur. Ceram. Soc.*, 2004, **24**, p 2055–2059
20. H. Awaji and Y. Sakaida, V-notch Technique for Single-Edge Notched Beam and Chevron Notch Methods, *J. Am. Ceram. Soc.*, 1990, **73**, p 3522–3523
21. H. Awaji, S.M. Choi, and D.D. Jayaseelan, Indirect Estimation of Critical Frontal Process-Zone Size Using a Single-Edge V-Notched-Beam Technique, *J. Ceram. Soc. Japan*, 2001, **109**, p 591–595